Study of end effects on the performance of the linear switched reluctance motor

Garcia Amorós J.[1] , Andrada Gascón P.[2]

[1] Departament d'Enginyeria Electrònica, Eléctrica i Automàtica
E.T.S.E., Universitat Rovira i Virgili
Avinguda Països Catalans, 26, 43007 Tarragona, Spain
Tel.:+34 977 559695, fax:+34 977559605
E-mail: jordi.garcia-amoros@urv.cat

[2] **GAECE.** Grup d'Accionamients Elèctrics amb Commutació Electrònica
Departament d'Enginyeria Elèctrica, EPSEVG-UPC
Víctor Balaguer s/n, 08800 Vilanova i la Geltrú, Spain
Tel.:+34 938967732; fax: +34 938967700
E-mail: andrada@ee.upc.edu

Key words

Finite element analysis, linear switched reluctance machine, end effects, analytical modelling

Abstract

The Switched reluctance motor (SRM) has been widely studied using two-dimensional finite element software packages, which have proven an effective approach for analysing SRM performance. However, end effects are not included in 2D FEA even though these effects can increase unaligned inductance by up to 20-30% [1], as the shorter the machine, the higher the increase. The results of this are a reduced energy conversion area predicted by 2D FEM and, therefore, lower performance calculations. End effects appear at the end of the lamination stack and are basically the consequence of extra flux linkages produced at the head or the end of the winding. This extra flux produces an axial fringing flux that, along with the steel imaging effect of the laminations, contributes to increasing these effects. The purpose of this paper is to study the end effects in a double-sided linear switched reluctance motor (LSRM). End effects in 2D FEA are taken into account by means of the end-effects coefficient, K_{ee} , [2] dependent of the current density (J) and position (x), given by:

$$\psi_{3D} = K_{ee} \cdot \psi_{2D}$$

$$L_{3D} = K_{ee} \cdot L_{2D}$$

Where Ψ_{2D} and L_{2D} are the flux linkage and the inductance obtained in 2D FEA [3] and Ψ_{3D} and L_{3D} are the 3D flux linkage and the inductance approaches that account for the end effects and are most similar to the measured values. The end-effects coefficient, K_{ee}, is defined as:

$$K_{ee} = \left(1 + \frac{L_{end} \cdot K_{si}}{L_{2D}}\right) \cdot K_f$$

Where, L_{end} is the end-winding inductance, K_{si} is a factor that affects L_{end} due to the steel imaging effect and K_f is the axial fringing factor. K_{si} can usually be omitted (K_{si} = 1) since its effect on L_{end} is generally less than 2%. The axial fringing flux is due to the tendency of the magnetic flux to bulge out in axial direction. This effect depends on the translator position and is stronger when the poles are fully unaligned (x=0) and weaker when they are completely aligned (x=S), where $S = Ts/2$ Therefore the axial fringing factor can be fitted by:

$$K_f(x) = 1 + \frac{2 \cdot g + l_s \cdot \left(1 + \cos\left(\pi \cdot x / S\right)\right)}{2 \cdot L_W}$$

End-winding inductance, $L_{end,}$ can be analytically deduced from Fig. 1 or can be computed by means of an axis-symmetrical 2D finite element model.

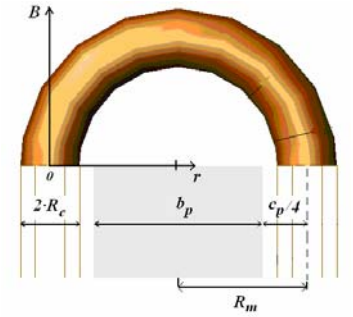

Fig. 1: Geometrical parameters for L_{end} calculation

End-winding inductance can be analytically obtained by considering end winding as a straight group of wires of the same length placed at a distance R_m from the steel core by means of the following equation:

$$L_{end} = k \cdot N_1^2 \cdot \mu_0 \cdot (b_p + \frac{c_p}{2}) \cdot \ln\left(\frac{\sqrt{\pi} \cdot (b_p + \frac{c_p}{2})}{e^{-\frac{1}{4}} \cdot \sqrt{c_p \cdot l_p \cdot k_v}}\right)$$

End-winding inductance can be calculated using a 2D FEM axis-symmetric solver by means of the model shown in Fig. 2. Each wire is considered an independent circuit. The end-winding inductance per phase is computed using the following expression:

$$L_{end} = 2 \cdot k \cdot \sum_{i=1}^{N_1} \left(L_i + \sum_{j=1}^{N_1} M_{i,j}\right)$$

Where L_i is the self inductance from i-wire and M_{ij} is the mutual inductance between wires i and j obtained by:

$$L_i = \frac{1}{I_i^2} \cdot \iint J_i \cdot A \cdot dS$$

$$M_{i,j} = \frac{1}{I_i} \cdot \oint_j \overline{A_j} \cdot dl$$

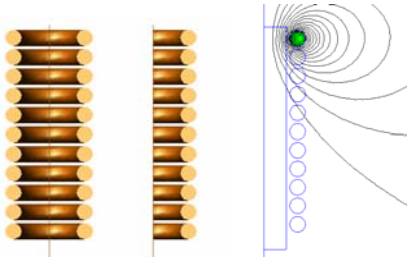

Fig. 2: Axis-symmetric FEM model for computing L_{end}.

Where $\overline{A}_j$ is the average magnetic potential over the surface S_j obtained by:

$$\overline{A}_j = \frac{1}{S_j} \cdot \iint_{S_j} A \cdot dS$$

Magnetization curves, flux linkage versus current for the different positions of the translator, are obtained by 2D FEA. Fig. 3 shows the flux lines for the aligned and unaligned positions of the LSRM.

.

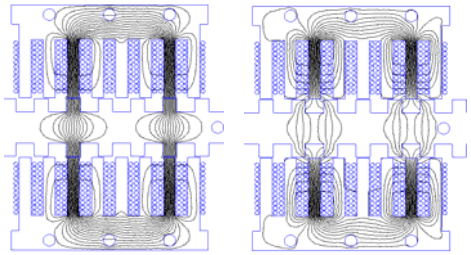

(a) (b)

Fig. 3: Flux plots from 2D FEM analysis of the LSRM a) Aligned b) Unaligned

The LSRM was tested in order to evaluate the results obtained by means of the proposed procedure. A test setup was built to perform the experimental measurements (Fig. 4). The flux linkage–current curves for aligned and unaligned position were obtained following the procedure described in [4].

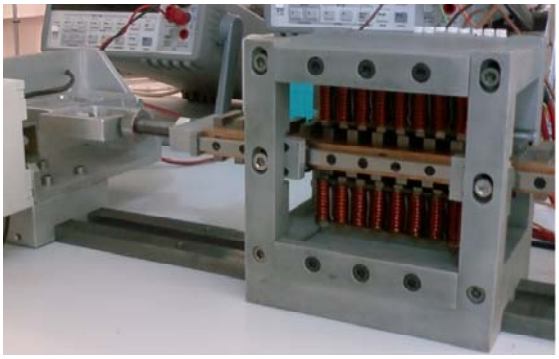

Fig.4. View of the test setup and of the double-sided LSRM

The propulsion force, including end effects, is obtained by:

$$F_{x,3D}(I) = \left. \frac{\partial W'_{3D}(x,I)}{\partial x} \right|_{I=Ctn}$$

Where the co-energy (W'_{3D}), knowing (Ψ_{3D}), is calculated using the well-known expression:

$$W'_{3D}(x_i, I) = \int_o^I \psi_{3D}(x,i) \cdot di \Big|_{x_i=Ctn}$$

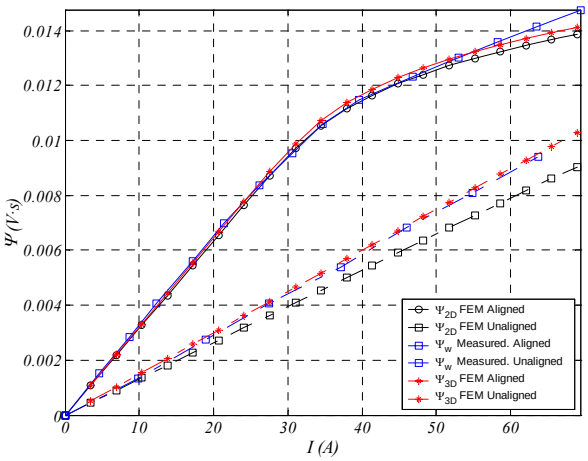

Fig. 5. Ψ_{2D}, Ψ_{3D} and measured flux linkage vs. current for aligned and unaligned position

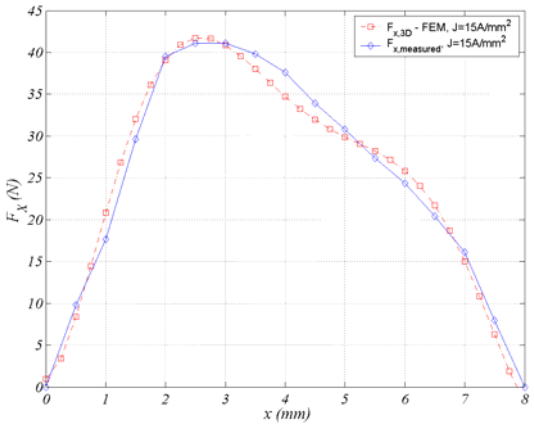

Fig. 6. 3D and measured propulsion force.

The comparison between the results obtained with the proposed procedure and the experimental test of magnetization curves (Ψ_{3D} *vs.* I) in the aligned and unaligned positions and propulsion force are plotted in Fig. 5 and Fig. 6 respectively. Then, it can be concluded that the results of this approach closely coincide with experimental measurements.

Acknowledgements

This research was supported by the Spanish Ministry of Education and Science and the ERDF (DPI2006-09880).

References

[1] T.J.E Miller, "Optimal Design of Switched Reluctance Motors". IEEE Transactions on Industrial Electronics, vol. 49, no. 1, pp. 15-27, Feb 2002

[2] A. Matveev, V. Kuzmichev, and E. Lomonova, "A new comprehensive approach to estimation of end-effects in switched reluctance motors", Proceedings ICEM2002, Bruges, Belgium, August 2002

[3] D.C. Meeker, Finite Element Magnetics Method. Version 4.2 *FEMM4.2* .15 May 2008 (*http://femm.foster-miller.net*)

[4] H. Bausch, K. Kanelis, "Feedforward Torque Control of a Switched Reluctance Motor Based on Static Measurement" ETEP, vol. 7, no. 6, pp. 373-380, November/December 1997.